Figure 3. Electron density map of thymine from the ab initio MO calculation. Note that the z-axis is about 2° out of the C–H bond direction when $\phi = 0°$. Contours at 0.05 $e^- \, A^{-3}$; maximum contour at 1.0 $e^- \, A^{-3}$.

dipolar interactions with protons on the reorientating methyl group ($\tau_c = 3 \times 10^{-12}$ s at 295 K). Therefore, if motion occurs at an N–H site, it must have a correlation time of less than 2×10^{-15} s (rms angle 12°) to yield a T_1 value of greater than 4000s.

Because this correlation time is implausible, we performed ab initio molecular orbital calculations[9] to see if the calculated static ^{2}H EFG tensors of thymine-*methyl-d3* could explain the large asymmetry parameter. The static EFG tensors of toluene-*methyl-d3* were also calculated, because the methyl group is also adjacent to an aromatic ring, but the observed asymmetry parameter, in contrast to that of thymine, is very small (less than 0.02).[10]

Figure 2a shows the calculated angular dependence of the deuterium quadrupole coupling constant (QCC) with respect to methyl group orientation for thymine and toluene. We note that for thymine with a dihedral angle of zero, the deuteron–exocyclic oxygen internuclear distance is only 2.436 Å. The atomic charge (Mulliken) on the exocyclic oxygen is 0.59 e^-. This value is in good agreement with UPS result[11] and other ab initio calculations.[12] From a point charge model, the charge at the oxygen site creates an EFG component of –2.5 kHz along the C–H bond vector of thymine methyl group. As seen in electron density map shown in Figure 3, a point charge model does not fully account for the electron density in the oxygen p-orbitals that lie close to the methyl deuteron site. A more exact calculation involving integration over all occupied molecular orbitals of the thymine molecule gives the deuterium QCCs shown in Figure 2a. The 8-kHz reduction in QCC is noteworthy for the deuterium closest to the exocyclic oxygen site, i.e., $\phi = 0°$. The effect of the exocyclic oxygen on the EFG is also seen in the orientation of z-axis, as shown in Figure 2b. We note that the aromatic π-electrons do not affect the deuterium QCC or the z-axis orientation in toluene to nearly the same extent as the exocyclic oxygen of thymine. The calculated asymmetry parameters of the static EFG tensors of both thymine and toluene are about 0.05. Following the con-

vention $|q_{zz}| \geq |q_{yy}| \geq |q_{xx}|$, the calculations showed, for both molecules, that the y-axis of the deuterium EFG is normal to the C_{ring}–C_{methyl}–D plane while the x-axis lies in the C_{ring}–C_{methyl}–D plane.

Since the hydrogen positions of the methyl group are unknown in the thymine crystal,[15] the space-averaged (C_3 jumps) ^{2}H EFG tensor is calculated based upon the ab initio results (Figure 2), varying the dihedral angle ϕ from 0° to 60°. At $\phi = 0°$, 20°, 40°, and 60°, the calculated values of the asymmetry parameter are 7%, 5%, 4%, and 3%, respectively. So a dihedral angle of less than 20° in thymine explains the experimentally obtained asymmetry parameter. On the other hand the calculated asymmetry parameters of the space-averaged ^{2}H EFG tensor for toluene are always less than 1% because the static EFG is nearly independent of ϕ. We believe that because a large asymmetry parameter is calculated over a large range of dihedral angle, that axially asymmetric spectra of the thymine moiety will be commonly seen.[18]

This study illustrates that reliable analysis of ^{2}H line shapes requires careful consideration of both the dynamic and static factors that affect the EFG tensor. In case of thymine-*methyl-d3*, the large ^{2}H methyl asymmetry parameter is caused by the negative charge density on the exocyclic oxygen, rather than motional narrowing.

(15) Ozeki, K.; Sakabe, N.; Tanaka, J. *Acta Crystallogr., Sect. B* **1969**, *25*, 1038.

(16) Gaussian-82 by: Binkley, J. S.; Frisch, M. J.; DeFrees, D. J.; Raghavachari, K.; Whitesides, R. A.; Schelgel, H. B.; Fluder, E. M.; Pople, J. A. Carnegie-Mellon University, 1984.

(17) Kern, C. W.; Matcha, R. L. *J. Chem. Phys.* **1968**, *49*, 2081.

(18) An axially asymmetric ^{2}H powder pattern has been reported[19] for hexamethylbenzene at 130 K. Ab initio and point charge model calculations show that the static ^{2}H EFG in o-xylene is reduced by ca. 4 kHz because of the 0.16 e^+ charge on the nearest hydrogen of neighboring methyl group. We therefore suggest that charge density on neighboring hydrogens is in part responsible for the asymmetric powder pattern observed[19] for hexamethylbenzene. It is also possible that rapid small-amplitude motions of the molecule may contribute to the anisotropy of the EFG in this case.

(19) Schwartz, L. J.; Meirovitch, E.; Ripmeester, J. A.; Freed, J. H. *J. Phys. Chem.* **1983**, *87*, 4453.

Di-π-methane-like Photorearrangement of Dimesityl(mesitylethynyl)borane: Synthesis, Structure, and Aromaticity of Trimesitylborirene[1]

John J. Eisch,*[†] Babak Shafii,[†] and Arnold L. Rheingold[‡]

Department of Chemistry
The State University of New York at Binghamton
Binghamton, New York 13901
Department of Chemistry, The University of Delaware
Newark, Delaware 19711

The capacity of tricoordinate boron to engage in π-bonding with adjacent unsaturated carbon is evident in the properties of boracyclopolyenes. The heightened chemical reactivity of pentaarylboroles[2] and the relative chemical stability of heptaarylborepins[3] can be ascribed to the Hückel antiaromaticity of the former[4] and the Hückel aromaticity of the latter.[5] In addition, aromatic anions have been generated from both the boracyclo-

(9) Gaussian-82 and the associated properties package was used to calculate the ^{2}H EFG in molecular and principal axis systems.[16] An interactive matrice manipulation program (Speakeasy) was used for determining the orientation of the EFG tensor. A Gaussian basis set (6-31G) was used for the results reported here. One calculation of toluene was done with p- and d-orbitals on the methyl hydrogen atoms; relative to (6-31G) basis set results, all electric field gradients were reduced by roughly the same factor, 0.9, while the orientation of the EFG tensor was unchanged. No corrections were made for C–H stretching vibrational effects.[17]
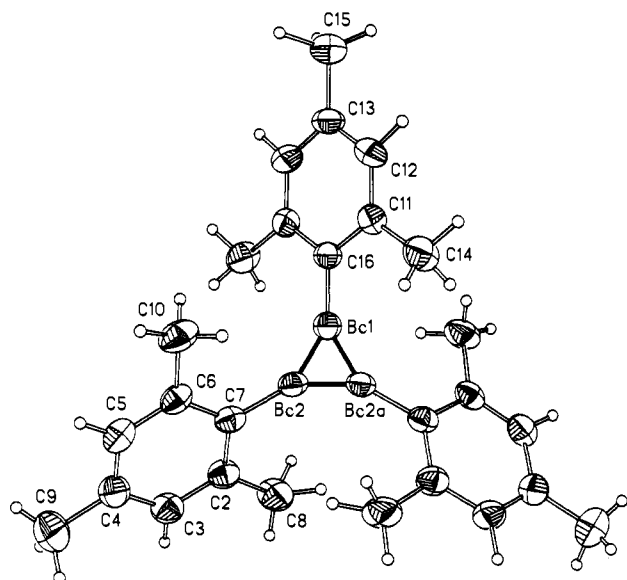
(10) Eckman, R. *J. Chem. Phys.* **1983**, *79*, 524.

(11) Palmer, M. H.; Wheeler, J. R.; Kwiatowski, J. S.; Lesyng, B. *J. Mol. Struct.* **1983**, *92*, 283.

(12) Scanlan, M. J.; Hillier, I. H.; MacDowell, A. A. *J. Am. Chem. Soc.* **1983**, *105*, 3568.

(13) Sarkar, S. K.; Sullivan, C. E.; Torchia, D. A. *J. Biol. Chem.* **1983**, *258*, 9762.

(14) Hiyama, Y.; Silverton, J. V.; Torchia, D. A.; Gerig, J. T.; Hammond, S. J. *J. Am. Chem. Soc.* **1986**, *108*, 2715.

†The State University of New York at Binghamton.
‡The University of Delaware.

(1) Part 9 in the series, Bora–Aromatic Systems. Part 8: Eisch, J. J.; Galle, J. E.; Kozima, S. *J. Am. Chem. Soc.* **1986**, *108*, 379.

(2) Eisch, J. J.; Galle, J. E.; Kozima, S. *J. Am. Chem. Soc.* **1986**, *108*, 379.

(3) Eisch, J. J.; Galle, J. E. *J. Am Chem. Soc.* **1975**, *97*, 4436.

(4) Breslow, R.; Chang, H. W. *J. Am. Chem. Soc.* **1961**, *83*, 3728; **1963**, *85*, 2033.

(5) Streitwieser, A., Jr. *Molecular Orbital Theory for Organic Chemists*; Wiley: New York, 1961; pp 256–304.

Figure 1. The molecular structure and labeling scheme for trimesitylborirene drawn with arbitrary radius hydrogen atoms. The crystallographic 2-fold axis is vertical in the plane of the figure. BC(1)–BC(2) 1.416 (6), BC(2)–BC(2a) 1.417 (7), BC(1)–C(16) 1.470 (7), BC(2)–C-(7) 1.506 Å; BC(1)–BC(2)–BC(2a) 60.0 (2)°, BC(2)–BC(1)–BC(2a) 60.0 (4)°. Torsion angles to the plane of BC(1)BC(2)BC(2a): C(2)–C(7) ring, 37.0 (4)°; C(11)–C(16) ring, 45.5 (4)°.
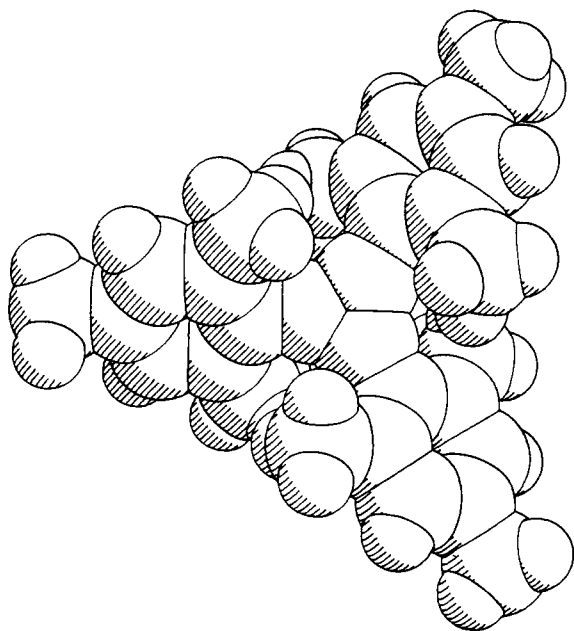

Figure 2. Space-filling representation of trimesitylborirene (2-fold axis horizontal) revealing the methyl group environment above and below the boracyclopropene ring.

pentadiene[2,6] and boracyclohexadiene systems.[7] In attempts to determine whether such boron–carbon π-bonding is also operative in the boracyclopropene ring, several research groups have generated[8] and isolated[9] boracyclopropenes (borirenes) and charac-

terized them by analytical and spectral data. However, no detailed structural information exists on the extent of π-electron delocalization in such borirenes.

In view of this situation, we have undertaken the synthesis of a solid borirene, upon which to perform an X-ray crystallographic analysis and thus to determine the bond distances in the three-membered ring. Here we wish to report that we have synthesized trimesitylborirene (**2**) by the photorearrangement of dimesityl-(mesitylethynyl)borane (**1**)[10] and have determined the structure of **2** by X-ray crystallography.

The photorearrangement of **1** was conducted in a benzene solution containing pyridine, and the irradiation was continued at 300 nm for 16 h (eq 1).[11] The borirene **2** is a colorless solid
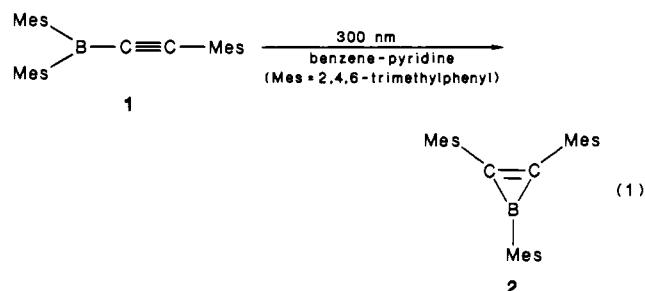
that melts at 217–218 °C after recrystallization from hexane.[12] It can be heated at 250 °C for 5 min in the air without undergoing decomposition. Its ultraviolet spectrum has its long-wavelength maximum at 280 nm in hexane, 312 nm in benzene, and 350 nm in pyridine. The borirene forms a labile complex with pyridine and a more stable, isolable yellow complex with 4-(dimethylamino)pyridine. Heating **2** with glacial acetic acid readily produces (Z)-1,2-dimesitylethene.

The result of the X-ray crystallographic analysis has proved to be most informative (Figures 1 and 2):[13] within experimental error, the three-atom ring forms an equilateral triangle with all the bond distances at 1.42 Å. Indeed, whether the ring sites are occupied by a given boron or a given carbon cannot be discerned.[13]

(6) Herberich, G. E.; Buller, G.; Hessner, B.; Oschmann, W. *J. Organomet. Chem.* **1980**, *195*, 249.

(7) Ashe, A. J., III; Meyers, E.; Shu, P.; von Lehmann, T.; Bastide, J. *J. Am. Chem. Soc.* **1975**, *97*, 6865.

(8) (a) Eisch, J. J.; Gonsior, L. J. *J. Organomet. Chem.* **1967**, *8*, 53. (b) Eisch, J. J.; Becker, H. P. *J. Organomet. Chem.* **1979**, *171*, 141. (c) Eisch, J. J.; Shen, F.; Tamao, K. *Heterocycles* **1982**, *18*, 245.

(9) (a) van der Kerk, S. M.; Budzelaar, P. H. M.; van der Kerk-van Hoof, A.; van der Kerk, G. J. M.; Schleyer, P. v. R. *Angew. Chem.* **1983**, *95*, 61. (b) Habben C.; Meller, A. *Chem. Ber.* **1984**, *117*, 2531. (c) West, R.; Pachaly, B. *Angew. Chem.* **1984**, *96*, 96. (d) Berndt, A.; Pues, C. *Angew. Chem.* **1984**, *96*, 306.

(10) Compound **1** was synthesized by the following sequence: (a) fluoro-(dimesityl)borane (Brown, H. C.; Dodson, V. H. *J. Am. Chem. Soc.* **1957**, *79*, 2302) was synthesized, (b) Me$_3$Si—C≡C—SO$_2$Ar (Bhattacharya, S. N.; Josiah, B. M.; Walton, D. R. M. *Organomet. Chem. Synth.* **1970–1971**, *1*, 145) was treated with mesitylmagnesium bromide and the Me$_3$Si—C≡C—Mes then treated with CsF to yield mesitylethyne, (c) mesitylethyne was treated with *n*-butyllithium and the resulting reagent coupled with floro(dimesityl)borane; **1** melts at 124–125 °C. IR (CCl$_4$) 3000 (s), 2125 (vs), 1605 (s) cm^{-1}; MS (70 eV), *m/e* (relative intensity) 392 (66), 272 (50), 257 (100); UV (hexane) long-wavelength absorption at 338 nm.

(11) The photoreaction was conducted in Rayonet Reactor, Model RPR (low-pressure mercury lamps of 300-nm wavelength), and the irradiation was performed on degassed reagents and anhydrous solvents under argon.

(12) Compound **2** displays these other spectral properties: (a) IR (CCl$_4$) 3000 (s), 1610 (s), 1440 (s), 1100 (s) cm^{-1}; (b) MS (70 eV), *m/e* (relative intensity) 392 (48), 272 (43), 257 (100); (c) ^{1}H NMR(CCl$_4$) δ 6.9 (s, 6 H), 2.2 (s, 15 H), 2.0 (s, 12 H).

(13) For C$_{29}$H$_{33}$B (293 K): monoclinic, C2/c, a = 9.734 (2) Å, b = 13.303 (4) Å, c = 19.125 (5) Å, β = 105.61 (2)°, V = 2385 (1) Å^3, Z = 4, μ (Mo Kα) = 0.56 cm^{-1}, D(calcd) = 1.092 g cm^{-3}. A colorless crystal (0.16 × 0.24 × 0.32 mm), the best of several screened, was only a moderately good diffractor which limited data collection to 2θ = 45° (Nicolet R3m/μ, Mo Kα radiation). Of 1538 independent, systematically present reflections (R$_{int}$ = 1.70%), 1094 were observed at the 2.5σ(F$_o$) level. A combination of direct methods and difference Fourier syntheses located all atoms. The molecule contains a crystallographic 2-fold rotational axis passing through atoms BC(1), C(13), C(15), and C(16) and the bisector of the BC(2)–BC(2a) vector. (Of necessity the C(15) methyl group hydrogen atoms are disordered; all six half-occupancy positions were located.) The centrosymmetric space group, C2/c, was originally suggested statistically and later confirmed by the chemically rational and computationally stable solution and refinement of the structure. An original assignment of boron to the unique boracyclopropene ring position and carbon to the other two symmetry-related positions led to a conspicuous difference in thermal parameters; B refined to U = 0.028 (2) Å^2 and C to U = 0.064 (2) Å^2. A site occupancy refinement for B and C led to 0.580 (4) for B and 0.921 (4) for C; these values may be compared with the expected values ^{1}/$_3$B + ^{2}/$_3$C identity of 0.567 and 0.944. Therefore, these ring atoms are disordered in atom identity and labeled BC(1) and BC(2). All non-hydrogen atoms were anisotropic and all hydrogen atoms isotropic in the final refinement. R(F) = 7.1%, R(wF) = 7.3%, GOF = 1.337, Δ/σ = 0.091, and Δ(ρ) = 0.17 e Å^{-3}. All software: SHELXTL and P3 (Nicolet Corp., Madison, WI).

Since the carbon–carbon double bond in cyclopropene has a length of 1.304 (3) Å[14] and the boron–carbon bond in trivinylborane has a length of 1.558 Å,[14] it is evident that the carbon–carbon bond in **2** has been lengthened by 0.11 Å and the boron–carbon bond contracted by 0.14 Å. Therefore, these bond length changes strongly support the conclusion that the two π-electrons in the borirene ring are completely delocalized among the boron and carbon p-orbitals. Thus the ring can be viewed as having Hückel aromaticity, quite analogous to that of the triphenylcyclo-propenium cation.[15,16]

Acknowledgment. We acknowledge gratefully the support of the Air Force Office of Scientific Research, Air Force Systems Command, USAF, under Grant No. AFOSR-85-0108.

Supplementary Material Available: Tables of atom coordinates, bond distances and angles, and anisotropic thermal parameters (3 pages); listing of observed vs. calculated structure factors (10 pages). Ordering information is given on any current masthead page.

(14) Vilkov, L. V.; Mastryukov, V. S.; Sadova, N. D. *Determination of the Geometrical Structure of Free Molecules*; Mir: Moscow, 1983.

(15) Sundaralingam, M.; Jensen, L. H. *J. Am. Chem. Soc.* **1966**, *88*, 198.

(16) While one might consider that the disorder in the BC_2 ring would cast doubt on the claim of equality of the bond distances in the three-membered ring, the presence of an approximately equilateral array for the BC_2 atoms is supported by the nearly equivalent arrangement of the three mesityl rings. It is true that the crystallographic site symmetry could have accommodated an isosceles BC_2 array with a 0.26-Å difference in the B–C and C–C bond distances. However, if the bond distances were so different, the mesityl rings would have chosen some other torsional arrangement: the adjacent mesityl groups on the supposed C=C bond would be expected to be twisted with their ring planes more toward the perpendicular to the plane defined by the BC_2 array than would be the mesityl appended to boron. That the three mesityl groups have the same torsional angle with respect to the BC_2 plane means that the difference in the actual separations, C–C and B–C, cannot be anywhere nearly as large as such hypothetical, localized bonding description would require. It should be noted that ab initio molecular orbital calculations utilizing modified versions of GAUSSIAN 70 and GAUSSIAN 76 series of programs have been carried out on borirene, BC_2H_3, by using split valence 4-31G basis and estimating correlation energies through application of Møller–Plesset second-order perturbation theory at the 4-31G basis set level. The calculated B–C bond length is 1.476 Å, and the C–C bond distance 1.347 Å. These calculations are at variance with our experimental findings. Cf.: Krogh-Jespersen, K.; Cremer, D.; Dill, J. D.; Pople, J. A.; Schleyer, P. v. R. *J. Am Chem. Soc.* **1981**, *103*, 2589.

High-Temperature Superconductivity in Y–Ba–Cu–O: Identification of a Copper-Rich Superconducting Phase

Angelica M. Stacy,* John V. Badding,
Margret J. Geselbracht, William K. Ham, Gary F. Holland,
Renata L. Hoskins, Steven W. Keller, Clark F. Millikan, and
Hans-Conrad zur Loye

Department of Chemistry, University of California and Materials and Chemical Sciences Division Lawrence Berkeley Laboratory, Berkeley, California 94720

Received March 10, 1987

For the past 15 years, advances in superconductivity have come about only slowly and even a 0.5 K increase in transition temperature was noteworthy. Until April 1986, the highest transition temperatures were near 23 K. At that time, Bednorz and Müller reported superconductivity in La–Ba–Cu–O compounds above 30 K.[1] Following this breakthrough, there were further studies of these phases and superconductivity was found also in similar solids containing Sr and Ca instead of Ba.[2–7] The superconducting phase

was identified as a layered perovskite $A_{2-x}B_xCuO_4$ with tetragonal symmetry, where $A = La^{3+}$ and $B = Ca^{2+}$, Sr^{2+}, or Ba^{2+}. The Sr compounds with $x = 0.15$ show the highest transition temperatures with T_c near 36 K.[5] These studies lead to the investigation of other ternary copper oxides and soon thereafter Chu and co-workers[8,9] found that compounds with a nominal composition of $Y_{1.2}Ba_{0.8}CuO_4$ could be prepared with superconducting transitions near 100 K. In contrast to the $La_{2-x}Sr_xCuO_4$ phases, the analogous $Y_{2-x}Ba_xCuO_4$ materials contain more than one phase. We report here the composition and properties of a superconducting phase containing Y, Ba, Cu, and O which is copper-rich compared with $Y_{1.2}Ba_{0.8}CuO_4$.

Chu and co-workers[8,9] and a number of other investigators[10–12] began to study $Y_{2-x}Ba_xCuO_4$ phases; our work[10] was motivated by the hope that the superconducting properties of $La_{2-x}Ba_xCuO_4$ could be tailored by substituting the smaller cation Y^{3+} for La^{3+}. It was almost beyond dreams to discover that some samples of nominal composition $Y_{2-x}Ba_xCuO_4$ superconducted above liquid nitrogen temperatures. However, it was evident from magnetic studies that only a small portion of the sample was superconducting and X-ray powder diffraction patterns indicated that no layered perovskite phases were present in the materials. The superconducting samples with nominal composition $Y_{1.2}Ba_{0.8}CuO_4$ are composed of at least two Y–Ba–Cu–O phases of different stoichiometries; a green phase and a black phase are easily distinguished under a light microscope. Unfortunately, due to the small crystallite size and extensive intergrowth, it has not been possible to separate the phases for analysis. In order to understand the chemistry of these materials, we synthesized and characterized $Y_{1-x}Ba_xCu_yO_z$ materials with various stoichiometries and have bracketed the stoichiometry of the superconducting phase.

Samples of nominal composition $Y_{1-x}Ba_xCu_yO_z$ with $0.15 < x < 0.55$ and $0.25 < y < 2$ were prepared by reacting stoichiometric ratios of Y_2O_3 (Alpha Products), $BaCO_3$ (Fisher Scientific), and CuO (Fisher Scientific). Simply firing mixtures of the solids at elevated temperatures yielded materials with considerable intergrowth of phases. A more uniform material was obtained by starting with an intimate mixture of finely divided particles. This was achieved when the reactants where dissolved first in nitric acid and the solution was evaporated to dryness. The nitrates were decomposed at 800 °C for 2 h and the resulting grey powders were ground in a mortar, pressed into $^1/_4$-in. pellets at 8000 psi, and fired for 4 h at 1100 °C under a flow of oxygen in Pt crucibles. The samples were cooled to room temperature in 1 h. Powder X-ray diffraction patterns, scanning electron microscope images, and microprobe analyses were obtained for all the samples synthesized. The fraction of superconducting phase in the samples was determined by measuring the magnetization when the samples were cooled in a field of 12.5 G in a SQUID magnetometer, i.e., by measuring the Meissner effect.

Our initial experiments began with compositions near $x = 0.4$ and $y = 0.5$, since this is the nominal composition of the materials which had been reported to superconduct above liquid nitrogen temperature. The best samples contained only 2% of a superconducting phase as determined by the Meissner effect. The powder patterns were quite complex and showed at least two sets

(4) Chu, C. W.; Hor, P. H.; Meng, R. L.; Gao, L.; Huang, Z. J.; Wang, U. Q. *Phys. Rev. Lett.* **1987**, *58*, 405.

(5) Cava, R. J.; van Dover, R. B.; Batlogg, B.; Rietman, E. A. *Phys. Rev. Lett.* **1987**, *58*, 408.

(6) Bednorz, J. G.; Muller, K. A.; Takashige, M. *Science (Washington, D.C.)*, in press.

(7) Panson, A. J.; Wagner, G. R.; Braginski, A. I.; Gavaler, J. R.; Janocko, M. A.; Pohl, G. C.; Talvacchio, J. *Appl. Phys. Lett.*, in press.

(8) Wu, M. K.; Ashburn, J. R.; Torng, C. J.; Hor, P. H.; Meng, R. L.; Gao, L.; Huang, Z. J.; Wang, Y. Q.; Chu, C. W. *Phys. Rev. Lett.* **1987**, *58*, 908.

(9) Hor, P. H.; Gao, L.; Meng, R. L.; Huang, Z. J.; Wang, Y. Q.; Forster, K.; Vassilious, J.; Chu, C. W. *Phys. Rev. Lett.* **1987**, *58*, 911.

(10) Bourne, L. C.; Cohen, M. L.; Creager, W. N.; Crommie, M. F.; Stacy, A. M.; Zettl, A. *Phys. Lett.*, in press.

(11) Sun, J. Z.; Webb, D. J.; Naito, M.; Char, K.; Hahn, M. R.; Hsu, J. W. P.; Kent, A. D.; Mitzi, D. B.; Oh, B.; Beasley, M. R.; Geballe, T. H.; Hammond, R. H.; Kapitulnik, A., unpublished results.

(12) Tarascon, J. M.; Greene, L. H.; McKinnon, W. R.; Hull, G. W. *Phys. Rev. Lett.*, in press.

*Author to whom correspondence should be addressed.

(1) Bednorz, J. G.; Müller, K. A. *Z. Phys.* **1986**, *B64*, 189.

(2) Uchida, S.; Takagi, H.; Kitazawa, K.; Tanaka, S. *Jpn. J. Appl. Phys. Lett.*, in press.

(3) Takagi, H.; Uchida, S.; Kitazawa, K.; Tanaka, S. *Jpn. J. Appl. Phys. Lett.*, in press.